ACS Photonics

pubs.acs.org/journal/apchd5

Article

Hybrid Optical and Diffusiophoretic Nanomanipulation Using All-Dielectric Anapole-Enhanced Thermonanophotonics

Ikjun Hong, Theodore Anyika, Chuchuan Hong, Sen Yang, and Justus C. Ndukaife*

Cite This: *ACS Photonics* 2023, 10, 4038–4044

Read Online

ACCESS | Metrics & More | Article Recommendations | Supporting Information

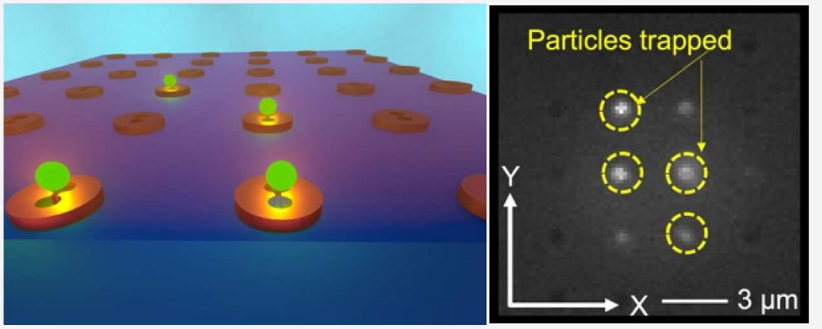

ABSTRACT: We present a noninvasive platform that combines the near-field optical gradient force from a nonradiating anapole nanoantenna with a diffusiophoretic force to achieve nanoscale particle transportation, trapping, and manipulation. Our approach utilizes a-Si-based nanocylinder supporting optical anapoles and serves as a nanoscale heat source at visible wavelengths, resulting in the generation of a diffusiophoretic force that enables the precise manipulation of nanoscale particles. These manipulations are performed in a water medium containing 10% poly(ethylene glycol) polymer molecules. Through experimental demonstrations, we successfully transport and manipulate a 300 nm PS bead on anapole arrays spaced at 2, 3, and 5 μm, using a low laser intensity of 0.2 mW/um^2. The synergistic integration of the optical gradient force and the photothermally induced diffusiophoretic force holds immense potential for advancements in nanoscience and life science by providing the means to exert control over nanosized objects.

KEYWORDS: *diffusiophoresis, anapole, nanotweezer, thermophoresis, electric field enhancement*

INTRODUCTION

Dynamic manipulation of a nanoscale particle is crucial to implement various applications such as nanorheology,[1] quantum photonics, and biophysics. For example, by studying the motion of a nanoscale particle within a medium, the nanorheology offers the capability to investigate the properties of the medium such as surface tension, viscosity, elasticity, and relaxation times. In the field of quantum photonics, one of the challenges faced is the precise positioning of quantum dots in a manner that maximizes the interaction between light and matter, thereby enabling the integration of a quantum source into a photonic nanobeam cavity.[2] On the other hand, in the realm of biophysics, the manipulation of a double-stranded DNA-linked micro- or nanobead holds significant biophysical interest, encompassing areas such as DNA elasticity, protein folding, and RNA folding.[3,4] Since then, the optical tweezer, a revolutionary tool that utilizes focused laser beams to trap and manipulate microscopic particles with precision, has been invented and widely adopted. Unfortunately, the width of the potential well generated by the conventional optical tweezer is limited to half of the wavelength, which corresponds to the scale of the diffraction limit of the laser. This limitation presents a challenge when attempting to trap and manipulate nanoscale particles using low-intensity illumination. To overcome the diffraction limit of the laser, plasmonic-based nanoantennas have been devised as a solution to enhance the near field intensity gradient, enabling to trap nanoscale particles.[5] The localized surface plasmon resonance, which is a collective oscillation of electrons on the metal's surface, can compress the wavelength well below the diffraction limit, thereby supporting a narrower potential well that can be utilized for trapping nanoscale particles. Despite the locally enhanced electric field provided by the plasmonic nanoantenna, the inherent Ohmic loss leads to photothermal-induced local temperature rise in the vicinity of the nanoantenna.[6,7] As a result, the particles within the medium experience buoyancy-driven thermal convection[6] or positive thermophoresis[8] occurring within the fluid-containing me-

Received: July 12, 2023
Published: September 29, 2023

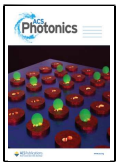

https://doi.org/10.1021/acsphotonics.3c00983
ACS Photonics 2023, 10, 4038–4044

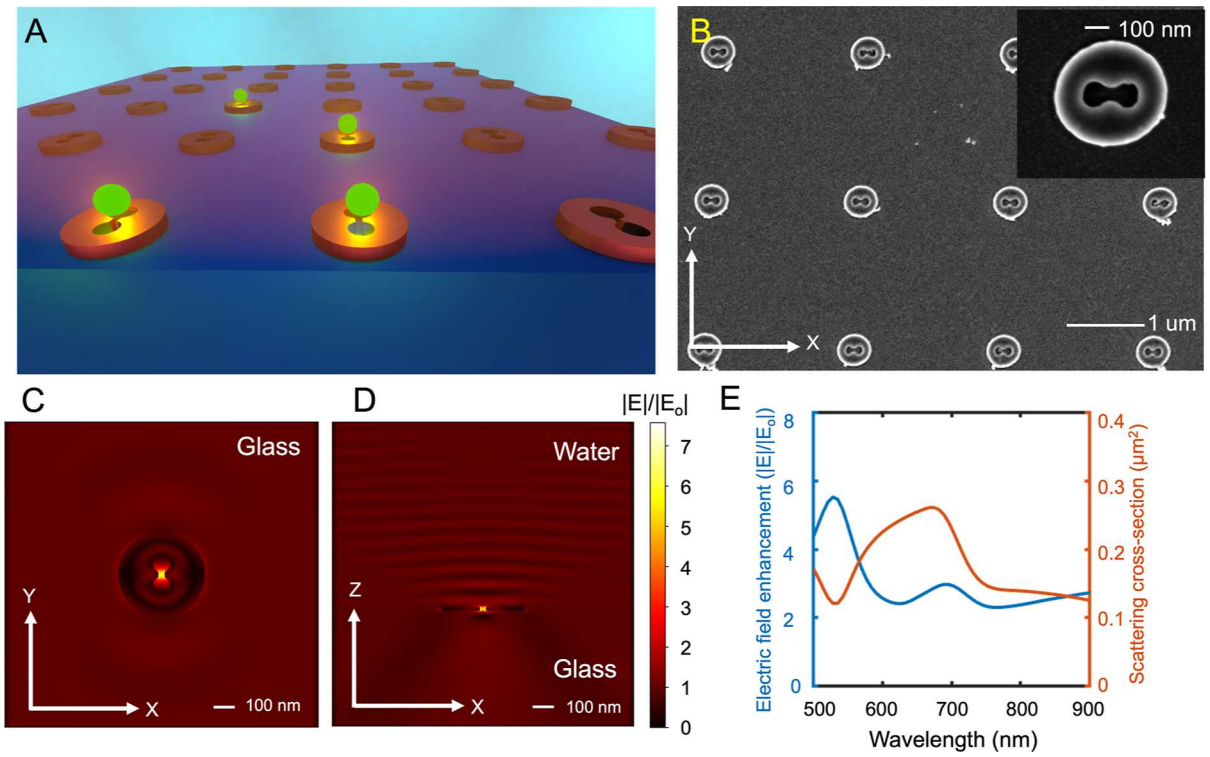

Figure 1. Designed array of anapole nanoantenna and the result of electromagnetic simulation. (A) Illustration of the designed anapole array with fluorescence labeled nanoparticles. (B) SEM image of fabricated anapole with a double nanohole aperture. (C) Distribution of electric field enhancement along the *XY* plane, at 27.5 nm above the glass substrate. (D) Distribution of electric field enhancement along the *XZ* plane, at the middle of the anapole disk on the glass substrate. (E) Simulation results of scattering cross-section and the electric field enhancement that the designed anapole can support.

dium. Positive thermophoresis exerts body forces away from high temperatures toward low temperatures, thereby hindering stable particle trapping at the plasmonic hotspots. The rise in the local temperature poses an obstacle to effectively trap and accumulate particles in the microfluidic channel. However, recent studies in the literature have begun to explore the utilization of thermal effects within the microfluidic channel to serve as a key component for particle trapping and accumulation.[9−15] Liu et al. have demonstrated the size-dependent enrichment of extracellular vesicles by optimizing various factors, including the chamber height, thermophoresis, diffusion, and buoyancy-driven toroidal convection.[16] In a demonstration by Jiang et al., the thermophobic and thermophilic behavior of particles was studied using an aperture incorporated with double nanoholes.[17] This study compared the stiffness of the trapped particles in different surfactant-dissolved media.

Here, we propose a method to trap, transport, and manipulate a single nanoscale particle in a poly(ethylene glycol) (PEG)-containing solution using a nonradiating anapole nanoantenna. The optical anapole is a state of multipoles, characterized by the presence of electric and toroidal dipole moments, in which the radiation from these moments is effectively canceled out due to their closely matched radiation patterns and opposite phase conditions.[18−21] This results in the trapping of light inside the supporting structure. In this study, our proposed platform for transporting and trapping nanoscale particles is to use the optical anapole in a PEG dissolved water medium. Under the illumination of 532 nm in wavelength, the anapole nanoantenna exhibits an enhanced electromagnetic field between the double nanoholes, which makes the electric field accessible to the medium and suspended particles. Since silicon is lossy at visible wavelengths, optical anapole enhances the absorption, thus making the anapole disk serve as a localized heat source. The induced thermal gradient causes the PEG molecules to experience a thermophoretic force directed from hot to cold, i.e., a repulsive positive thermophoresis drift due to the positive Soret coefficient of PEG molecules. In the steady state, a concentration gradient of PEG molecules is established and the spatial concentration can be calculated by solving the time-dependent equation given by $\frac{\partial c_{\mathrm{PEG}}}{\partial t} = \nabla\cdot(-D_{\mathrm{PEG}}\nabla c_{\mathrm{PEG}} - S_T^{\mathrm{PEG}} D_{\mathrm{PEG}} c_{\mathrm{PEG}} \nabla T)$, where the C_{PEG}, D_{PEG}, and $S_{\mathrm{T}}^{\mathrm{PEG}}$ are the concentration of PEG, diffusion coefficient of PEG, and Soret coefficient of PEG, respectively. Near the anapole nanoantenna, where the temperature is relatively high, the local concentration of PEG decreases, since the thermophoretic force repels the PEG to the cold region. While far from the anapole nanoantenna, the PEG concentration is comparable to the original concentration. The spatial depletion of PEG concentration makes the target particles experience the diffusiophoretic force, which is toward the center of the anapole nanoantenna. The rest of the article describes the theoretical design and experimental validation to address the tweezing and manipulation of nanoscale particles.

SIMULATION RESULTS

The strategy for trapping and manipulating nanoscale particles involves utilizing diffusiophoresis in conjunction with the near-field gradient force generated by an anapole nano disk. In this approach, an amorphous silicon (a-Si)-based nanodisk serves

https://doi.org/10.1021/acsphotonics.3c00983
ACS Photonics 2023, 10, 4038−4044

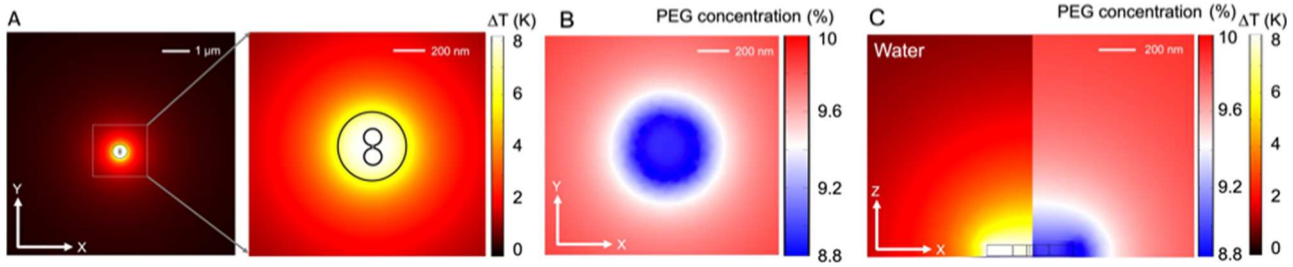

Figure 2. Simulation result of the local temperature distribution with a spatial distribution of PEG molecules. (A) Distribution of thermal simulation under 10 mW power with a spot diameter of 8 μm. The results of the thermal simulation show that the maximum temperature rise is approximately 8 K along the *XY* plane. (B) Distribution of PEG concentration along the *XY* plane, 50 nm above the anapole disk's surface. (C) Distribution of the thermal map and PEG concentration along the *XZ* plane, showing spatial depletion of PEG concentration where the local temperature increases.

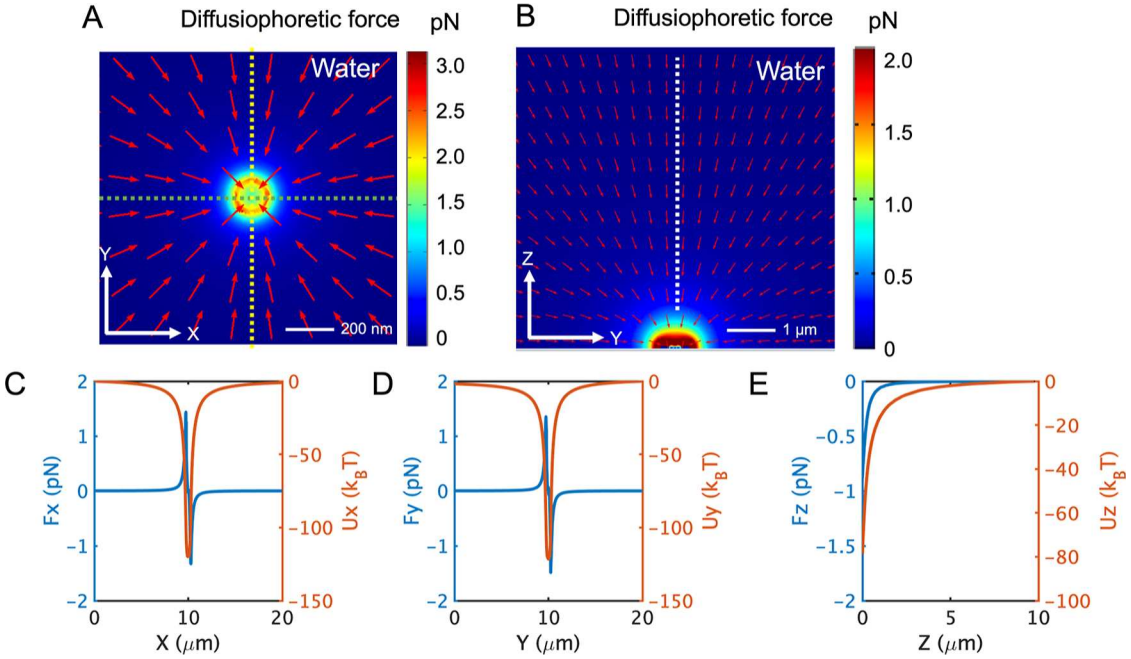

Figure 3. Diffusiophoretic force calculation. (A) Map of diffusiophoretic force along the *XY* plane shows that the force is toward to the center of the anapole nanoantenna. (B) Map of diffusiophoretic force along the *ZY* plane. (C,D) Calculated diffusiophoretic force and the potential along the *X*, *Y* direction as marked by blue and yellow dot line in (A). (E) Calculated diffusiophoretic force and potential along the *Z* direction are marked by a white dot line in (B).

to support an anapole at a wavelength of 532 nm. When illuminated with a laser at this wavelength, the a-Si disk induces localized temperature rise in the surrounding water medium due to its nonzero imaginary part of refractive index (see Figure S1 for details). In order to facilitate the access of the enhanced electric field to the medium, a double nanohole (DNH) aperture is created at the center of the a-Si based nanodisk. Also, we have studied the effect of the periodicity of the anapole array on the ability to trap particles and manipulate the position of single particles by varying the center-to-center spacing of the anapole array.

Figure 1A provides an illustration of our proposed system, depicting an array of silicon nanodisks with drilled DNHs. The green sphere represents a fluorescence-labeled nanoparticle that is trapped on top of the anapole nanoantenna through the combined effects of diffusiophoresis and the optical gradient force generated by the anapole state. The parameters of the a-Si nanocylinder, including its height and radius, were investigated through a parameter sweep. Finally, we determined the optimal values to be 55 nm for the height and 215 nm for the radius, while the gap size of the DNH structure was set at 45 nm, with each hole having a radius of 50 nm. The scanning electron microscopy (SEM) image of the fabricated sample is shown in Figure 1B, showing the 2 μm spacing between nanodisks. Figure 1C,D shows the distribution of electric field on the optimized radius and height of nanodisk along the *XY* and *XZ* planes. The electric field is confined and enhanced inside of double nanoholes. The local electric field is boosted by approximately eight times due to the anapole state, and the scattering is suppressed at the 532 nm wavelength, as described in Figure 1E. Under the illumination of 532 nm incidence, the anapole nanoantenna not only exhibits an enhanced electric field but also acts as the local temperature emitter.

The result of thermal simulation shows that the anapole antenna induces the local temperature rising under 532 nm illumination along the *xy* plane, as shown in Figure 2A. The locally induced temperature rise decay spatially away from the anapole nanoantenna, and the maximum temperature rising is estimated to be ~8 K under 0.2 mW/um^2 intensity of laser.

https://doi.org/10.1021/acsphotonics.3c00983
ACS Photonics 2023, 10, 4038−4044

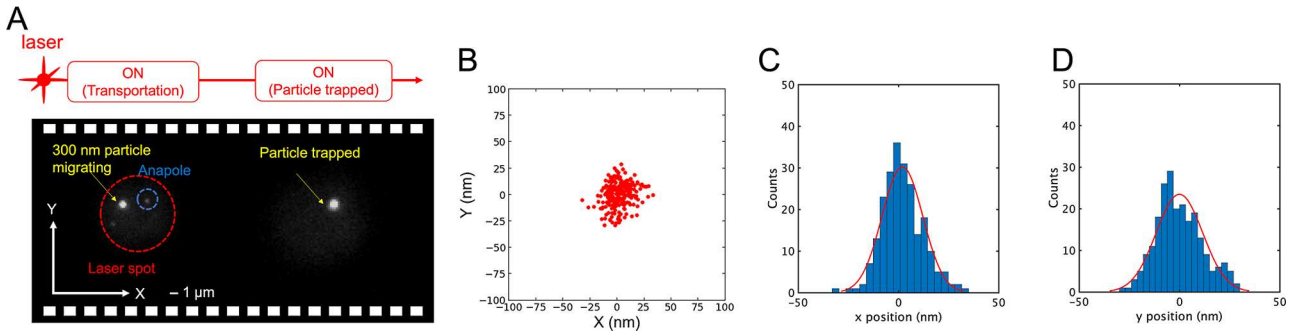

Figure 4. Particle trapping experiments. (A) 300 nm PS bead trapping experiment shows that the diffusing particle is trapped on the anapole nanoantenna. (B) Scatter plot shows the particle's trajectory when the particle is trapped on the anapole nanoantenna. The highest estimated stiffness along the *x*- and *y*-axis are 1.97 and 1.72 fN/nm under 0.2 mW/um^2 incident laser intensity, respectively. (C,D) Histogram of the trapped particle's position under 0.2 mW/μm^2 incident laser intensity along *x* and *y* direction, respectively. The red curve is the Gaussian fitting to estimate the trap stiffness.

The heat dissipation density was calculated by $Q = \frac{1}{2}Re(J^* \cdot E)$ where E is the electric field and J is the induced current density (see Figure S2 for details). After the local temperature gradient is established from the origin of the anapole nanoantenna, PEG molecules start to undergo a force toward the cold region from the hot region following the temperature gradient due to the inherent positive thermophoretic force. We can calculate the distribution of PEG molecules by solving the time-dependent equation given by $\frac{\partial c_{PEG}}{\partial t} = \nabla \cdot (-D_{PEG}\nabla c_{PEG} - S_T^{PEG} D_{PEG} c_{PEG} \nabla T)$, where the C_{PEG}, D_{PEG}, and S_T^{PEG} are the concentration of PEG, diffusion coefficient of PEG, and Soret coefficient of PEG, respectively (see S3 for details). Near the anapole nanoantenna, where the temperature is high, the local concentration of PEG decreases since the thermophoretic force repels the PEG to the cold region. Figure 2B,C shows the spatial distribution of PEG molecules along the *XY* and *XZ* planes in the steady state. The initial concentration of the PEG molecule is 10%, which is the same value used in the experiments. The concentration distribution reveals spatial contrast, with PEG molecules exhibiting a variation ranging from 10 to 8.8%. The simulation result shows the gradient of the concentration, and the local depletion of PEG concentration makes the nanoparticles experience the diffusiophoretic force, which is toward to the center of anapole nanoantenna.

The concentration gradient of PEG pushes the biocolloidal particle toward the region with low PEG concentration following the diffusiophoresis. Diffusiophoretic force can be calculated by $F = 3\pi\eta a D S_T \nabla T \propto a c_{peg} \nabla T$, where a is the particle diameter, η is the viscosity of fluid medium, D is the Brownian diffusion coefficient, S_T is the effective Soret coefficient of target particles, and c_{PEG} is the PEG concentration[22] (see Figure S4 for details).

Calculation indicates that the 300 nm particle can be transported to the center of the anapole nanoantenna with the assistance of diffusiophoresis, as described in Figure 3A,B. Figure 3A depicts the diffusiophoresis map above the *XY* plane at a height of 100 nm with the force generated by the temperature gradient (∇T). The calculated maximum force is approximately 3.1 pN for a 300 nm particle, with the force directing toward the region of higher temperature. In Figure 3B, the calculated force along the *XZ*-plane is mapped, causing the 300 nm particle to be pushed downward toward the nanoantenna region. Additionally, the diffusiophoretic forces and potential along the *X* and *Y* directions are calculated for a 300 nm polystyrene (PS) particle positioned 100 nm above the substrate. The maximum force along the *X* and *Y* directions is approximately ~1.4 pN, pointing toward the center of the anapole. The calculated potential reveals a value of ~ −125 k_BT, significantly higher than $-1k_BT$, indicating the likelihood of stable particle trapping. Furthermore, the calculation of force and potential along the *Z*-direction is presented in Figure 3E. The position of the 300 nm particle is parametrically swept from 250 nm above the substrate to 5000 nm. As the particle gradually moves away from the DNH, the force in the *Z*-direction (Fz) decays, suggesting that the trapped particle should remain confined close to the surface of the anapole disk.

EXPERIMENTAL RESULTS AND DISCUSSION

Single Particle Trapping. The colloidal nanoparticle experiences two forces: the optical force generated by the near field excited in the anapole and the diffusiophoretic force arising from the local depletion of PEG in the solution. The optical force can be estimated by using the Maxwell stress tensor method, which can be performed using commercially available Lumerical software. However, it is important to note that the optical force exerted by the near field from the anapole is relatively insignificant compared to the diffusiophoresis (refer to the Figures S5 and S7 for more details). The experimental results demonstrate that a 300 nm PS bead can be stably trapped under a 532 nm laser with a power of 10 mW and a spot size of 8 μm in diameter by using a 5 μm spacing of the anapole array (refer to Video S1 and Figure 4A).

Initially, the particle undergoes Brownian motion within the microfluidic channel. As the particle enters the region where the diffusiophoretic force becomes significant, the PS bead is transported to the top surface of the anapole, where the local temperature increase is the highest. The scatter plot in Figure 4B displays the position of the particle, demonstrating tight trapping under a laser intensity of 0.2 mW/μm^2. The PS bead is predominantly confined to the center, and the *X* and *Y* positions are depicted in Figure 4C,D as a histogram. A red line in Figure 4C,D represents the Gaussian fitting, allowing for the determination of the full-width and half-maximum to estimate the stiffness. The extracted stiffness along the *x* and *y* directions is determined to be 1.97 and 1.72 fN/nm, respectively, after correcting the effect of motion blur (see Figure S6 for details).

https://doi.org/10.1021/acsphotonics.3c00983
ACS Photonics 2023, 10, 4038−4044

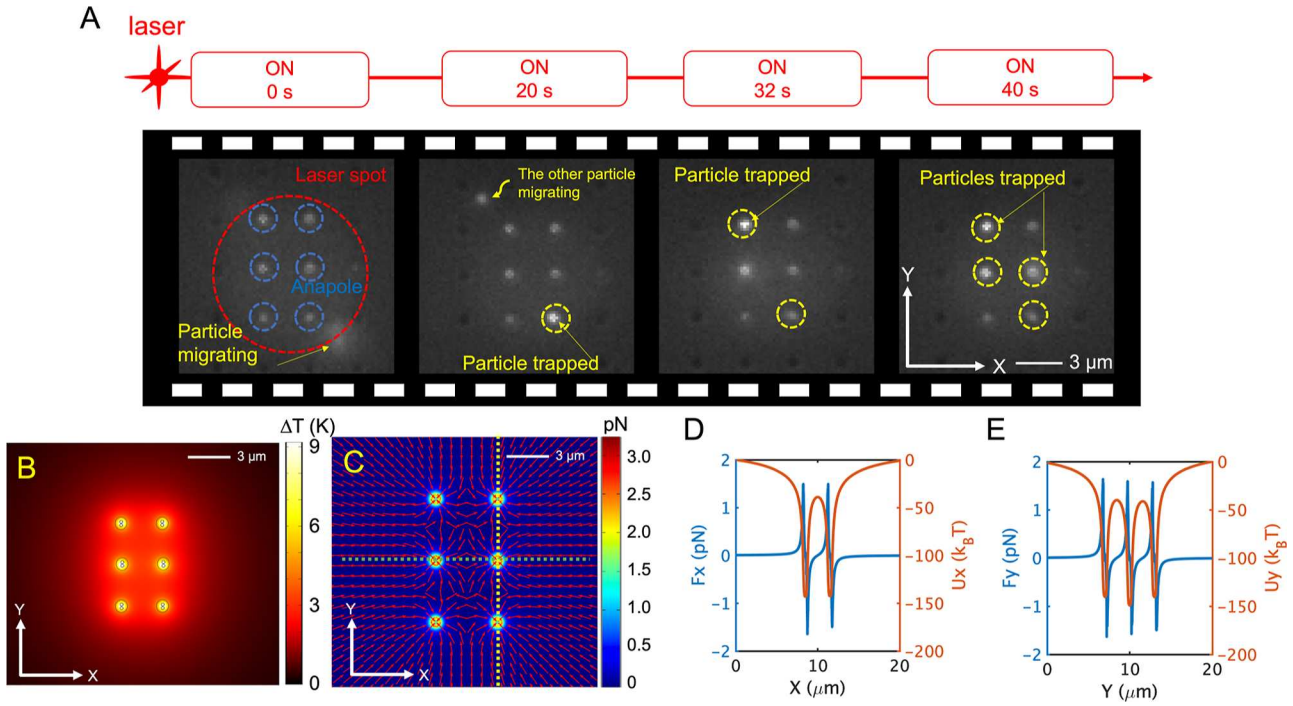

Figure 5. Multiparticle trapping experiments conducted using a 3 μm spacing of the anapole array. (A) Trapping experiment using 300 nm particles shows that the migrating particles move toward and get trapped on each anapole nanoantenna. (B) Result of thermal simulation on 2 by 3 array of anapole with a 3 μm spacing array of anapole. (C) Map of diffusiophoretic force on 50 nm above the anapole's surface along the *XY* plane. (D,E) Calculated diffusiophoresis and potential along the *X* and *Y* direction, marked by a green and yellow dot line in Figure 5C.

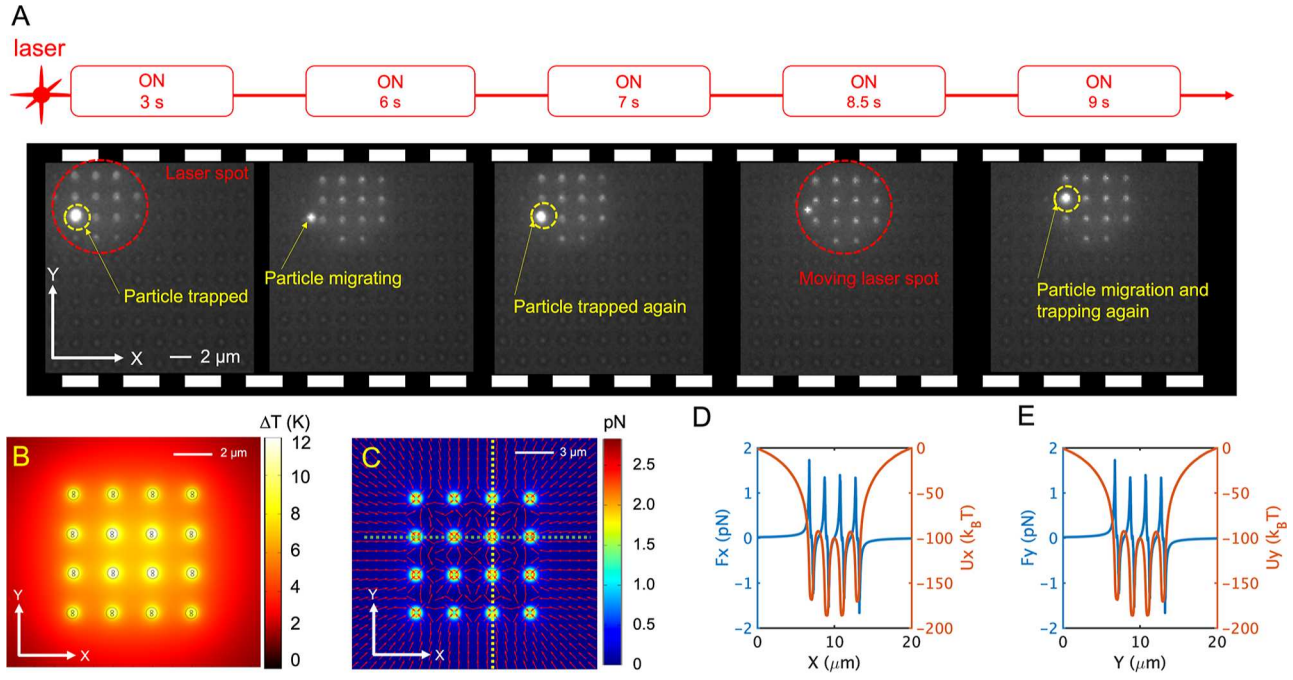

Figure 6. Manipulation of a 300 nm particle using a 2 μm spacing of the anapole array. (A) Sequence of video frames showing the manipulation of particle by moving a laser spot. (B) Result of thermal simulation on a 4 × 4 array of anapole with a 2 μm spacing array of anapole. (C) Map of diffusiophoretic force on 50 nm above the anapole's surface along the *XY* plane. (D,E) Calculated diffusiophoresis and potential along the *X* and *Y* direction, marked by a green and yellow dot line in Figure 6C.

Multiparticle Trapping. Subsequently, we conducted experiments to simultaneously trap multiple particles by using a 3 μm spacing of the anapole array. In Figure 5A, a continuous sequence of video frames demonstrates the successful trapping of multiple particles by the system (refer to Video S2). By focusing a 10 mW laser on the substrate with an 8 μm spot size in diameter, we observed the migration and tweezing action of fluorescence-labeled 300 nm PS beads. Additionally, both the thermal simulation and the fore calculations were performed based on a 2 by 3 array of

https://doi.org/10.1021/acsphotonics.3c00983
ACS Photonics 2023, 10, 4038−4044

anapoles. As we expected, the collective heating effect[23] makes the temperature further increase, compared to the result of a single structure, as previously described in Figure 2A. In addition, the diffusiophoretic force was also calculated, revealing that the direction of the force is toward the region where the local temperature increases, as depicted in Figure 5C. The forces along the X and Y directions, indicated by a green and yellow dotted line in Figure 5C, are further clarified in Figure 5D,E. By performing line integration along the X and Y directions, the diffusiophoretic potential was determined, as illustrated in Figure 5D,E. The potential well is found to be lower than $-150\ k_BT$, and a number of potential minima, totaling 2 and 3 along the X and Y directions, respectively, align with the number of anapole nanodisks present.

Manipulation of Particles. Additionally, to validate the manipulation capability of a 300 nm PS bead within our proposed system, we prepared a 2 μm spacing of an anapole array, as depicted in Figure 6A and Video S3. By moving the position of a laser spot across the anapole array, we observed the particle's behavior in relation to the laser spot. The 532 nm laser spot had a diameter of approximately 8 μm, and we observed the migration of a single particle, ultimately leading to its trapping on one of the anapole nanodisks. When we shifted the laser spot to another location, the particle exhibited migration toward the respective anapole. The particles tend to get trapped at the anapole nanoantenna located near the circumference of the laser beam. This is because the first potential that the particles encounter after being transported by the diffusiophoretic force is provided by the outer anapole antenna. Figure 6A presents a sequence of video frames showcasing the dynamic manipulation and tweezing action of a single particle. Using the 2 μm spacing of the anapole array, we conducted thermal simulations and force calculations, as well (Figure 6B,C). The collective heating effect led to a further increase in temperature compared to the 3 μm spacing case with a temperature rise of approximately 12 K along the XY plane (Figure 6B). The diffusiophoretic force analysis revealed that the particle experienced a force toward the center of the anapole nanodisk (Figure 6C). The 2 μm spacing, which is comparable to the width of the diffusiophoretic potential, facilitated easy manipulation of the 300 nm particle, following the direction of diffusiophoresis. The force and potential plots are depicted in Figure 6D,E. Notably, due to the 2 μm spacing between the nanodisks, a finger-shaped potential well was formed, resulting in a decrease in local potential magnitude compared to that of a single structure or a 3 μm spacing array.

CONCLUSIONS

In summary, we have proposed and experimentally demonstrated a method for particle trapping and transportation at predefined sites by using a low-intensity laser (0.2 mW/um^2). Our approach leverages the local depletion of PEG molecules to induce diffusiophoresis, enabling efficient particle trapping and transportation. Furthermore, by engineering the spacing between the anapole array, we have achieved the simultaneous trapping of multiple particles and dynamic manipulation of particles to other intended locations. We strongly believe that our anapole system has significant potential in facilitating the precise positioning and manipulation of nanoscale particles. This system holds promise in various fields such as quantum photonics, nanorheology, and biophysics, offering new opportunities for advanced research and applications.

ASSOCIATED CONTENT

Supporting Information

The Supporting Information is available free of charge at https://pubs.acs.org/doi/10.1021/acsphotonics.3c00983.

Single-particle trapping (MP4)
Multi-particle trapping (MP4)
Particle manipulation (MP4)
Ellipsometry result of the deposited a-Si; COMSOL simulation for the temperature rising; COMSOL modeling for the spatial distribution of PEG molecules; COMSOL modeling for the diffusiophoretic force; optical force calculation exerted on a 300 nm PS bead; correction function for the motion blur; and optical potential as a function of laser intensity (PDF)

AUTHOR INFORMATION

Corresponding Author

Justus C. Ndukaife − *Vanderbilt Institute of Nanoscale Science and Engineering, Vanderbilt University, Nashville, Tennessee 37235, United States; Department of Electrical and Computer Engineering, Department of Mechanical Engineering, and Center for Extracellular Vesicles Research, Vanderbilt University, Nashville, Tennessee 37235, United States;* orcid.org/0000-0002-8524-0657; Email: justus.ndukaife@vanderbilt.edu

Authors

Ikjun Hong − *Vanderbilt Institute of Nanoscale Science and Engineering, Vanderbilt University, Nashville, Tennessee 37235, United States; Department of Electrical and Computer Engineering, Vanderbilt University, Nashville, Tennessee 37235, United States;* orcid.org/0000-0003-1275-7740

Theodore Anyika − *Vanderbilt Institute of Nanoscale Science and Engineering, Vanderbilt University, Nashville, Tennessee 37235, United States; Department of Electrical and Computer Engineering, Vanderbilt University, Nashville, Tennessee 37235, United States;* orcid.org/0000-0002-7722-0816

Chuchuan Hong − *Vanderbilt Institute of Nanoscale Science and Engineering, Vanderbilt University, Nashville, Tennessee 37235, United States; Department of Electrical and Computer Engineering, Vanderbilt University, Nashville, Tennessee 37235, United States;* orcid.org/0000-0002-1329-9385

Sen Yang − *Vanderbilt Institute of Nanoscale Science and Engineering, Vanderbilt University, Nashville, Tennessee 37235, United States; Interdisciplinary Materials Science, Vanderbilt University, Nashville, Tennessee 37235, United States;* orcid.org/0000-0002-0056-3052

Complete contact information is available at: https://pubs.acs.org/10.1021/acsphotonics.3c00983

Notes

The authors declare no competing financial interest.

ACKNOWLEDGMENTS

I.H., T.A., C.H., S.Y., and J.C.N. acknowledge financial support from the National Science Foundation NSF CAREER Award (NSF ECCS 2143836). Fabrication of the nanostructures was conducted at the Vanderbilt Institute of Nanoscale Science and Engineering cleanroom facility.

https://doi.org/10.1021/acsphotonics.3c00983
ACS Photonics 2023, 10, 4038−4044

REFERENCES

(1) Robertson-Anderson, R. M. Optical Tweezers Microrheology: From the Basics to Advanced Techniques and Applications. *ACS Macro Lett.* **2018**, *7* (8), 968−975.
(2) Yang, S.; Allen, J. A.; Hong, C.; Arnold, K. P.; Weiss, S. M.; Ndukaife, J. C. Multiplexed Long-Range Electrohydrodynamic Transport and Nano-Optical Trapping with Cascaded Bowtie Photonic Crystal Nanobeams. *Phys. Rev. Lett.* **2023**, *130* (8), 083802.
(3) Bustamante, C. J.; Chemla, Y. R.; Liu, S.; Wang, M. D. Optical Tweezers in Single-Molecule Biophysics. *Nat. Rev. Methods Primers* **2021**, *1* (1), 25.
(4) Chemla, Y. R. High-Resolution, Hybrid Optical Trapping Methods, and Their Application to Nucleic Acid Processing Proteins. *Biopolymers* **2016**, *105* (10), 704−714.
(5) Wang, K.; Schonbrun, E.; Steinvurzel, P.; Crozier, K. B. Trapping and Rotating Nanoparticles Using a Plasmonic Nano-Tweezer with an Integrated Heat Sink. *Nat. Commun.* **2011**, *2* (1), 469.
(6) Roxworthy, B. J.; Bhuiya, A. M.; Vanka, S. P.; Toussaint, K. C. Understanding and Controlling Plasmon-Induced Convection. *Nat. Commun.* **2014**, *5* (1), 3173.
(7) Baffou, G.; Girard, C.; Quidant, R. Mapping Heat Origin in Plasmonic Structures. *Phys. Rev. Lett.* **2010**, *104* (13), 136805.
(8) Gargiulo, J.; Brick, T.; Violi, I. L.; Herrera, F. C.; Shibanuma, T.; Albella, P.; Requejo, F. G.; Cortés, E.; Maier, S. A.; Stefani, F. D. Understanding and Reducing Photothermal Forces for the Fabrication of Au Nanoparticle Dimers by Optical Printing. *Nano Lett.* **2017**, *17* (9), 5747−5755.
(9) Hong, C.; Yang, S.; Ndukaife, J. C. Exosomes Trapping, Manipulation and Size-Based Separation Using Opto-Thermo-Electrohydrodynamic Tweezers. *Nanoscale Adv.* **2023**, *5* (11), 2973−2978.
(10) Anyika, T.; Hong, C.; Ndukaife, J. C. High-Speed Nanoscale Optical Trapping with Plasmonic Double Nanohole Aperture. *Nanoscale* **2023**, *15*, 9710−9717.
(11) Hong, C.; Yang, S.; Kravchenko, I. I.; Ndukaife, J. C. Electrothermoplasmonic Trapping and Dynamic Manipulation of Single Colloidal Nanodiamond. *Nano Lett.* **2021**, *21* (12), 4921−4927.
(12) Lin, L.; Peng, X.; Wei, X.; Mao, Z.; Xie, C.; Zheng, Y. Thermophoretic Tweezers for Low-Power and Versatile Manipulation of Biological Cells. *ACS Nano* **2017**, *11* (3), 3147−3154.
(13) Fränzl, M.; Cichos, F. Hydrodynamic Manipulation of Nano-Objects by Optically Induced Thermo-Osmotic Flows. *Nat. Commun.* **2022**, *13* (1), 656.
(14) Deng, J.; Tian, F.; Liu, C.; Liu, Y.; Zhao, S.; Fu, T.; Sun, J.; Tan, W. Rapid One-Step Detection of Viral Particles Using an Aptamer-Based Thermophoretic Assay. *J. Am. Chem. Soc.* **2021**, *143* (19), 7261−7266.
(15) Hong, C.; Ndukaife, J. C. Scalable Trapping of Single Nanosized Extracellular Vesicles Using Plasmonics. *Nat. Commun.* **2023**, *14*, 4801.
(16) Liu, C.; Zhao, J.; Tian, F.; Cai, L.; Zhang, W.; Feng, Q.; Chang, J.; Wan, F.; Yang, Y.; Dai, B.; et al. Low-Cost Thermophoretic Profiling of Extracellular-Vesicle Surface Proteins for the Early Detection and Classification of Cancers. *Nat. Biomed. Eng.* **2019**, *3* (3), 183−193.
(17) Jiang, Q.; Rogez, B.; Claude, J.-B.; Baffou, G.; Wenger, J. Quantifying the Role of the Surfactant and the Thermophoretic Force in Plasmonic Nano-Optical Trapping. *Nano Lett.* **2020**, *20* (12), 8811−8817.
(18) Savinov, V.; Papasimakis, N.; Tsai, D. P.; Zheludev, N. I. Optical Anapoles. *Commun. Phys.* **2019**, *2* (1), 69.
(19) Baryshnikova, K. V.; Smirnova, D. A.; Luk'yanchuk, B. S.; Kivshar, Y. S. Optical Anapoles: Concepts and Applications. *Adv. Opt. Mater.* **2019**, *7* (14), 1801350.
(20) Miroshnichenko, A. E.; Evlyukhin, A. B.; Yu, Y. F.; Bakker, R. M.; Chipouline, A.; Kuznetsov, A. I.; Luk'yanchuk, B.; Chichkov, B. N.; Kivshar, Y. S. Nonradiating Anapole Modes in Dielectric Nanoparticles. *Nat. Commun.* **2015**, *6* (1), 8069.
(21) Yang, Y.; Zenin, V. A.; Bozhevolnyi, S. I. Anapole-Assisted Strong Field Enhancement in Individual All-Dielectric Nanostructures. *ACS Photonics* **2018**, *5* (5), 1960−1966.
(22) Maeda, Y. T.; Tlusty, T.; Libchaber, A. Effects of Long DNA Folding and Small RNA Stem-Loop in Thermophoresis. *Proc. Natl. Acad. Sci. U.S.A.* **2012**, *109* (44), 17972−17977.
(23) Roxworthy, B. J.; Bhuiya, A. M.; Vanka, S. P.; Toussaint, K. C. Understanding and Controlling Plasmon-Induced Convection. *Nat. Commun.* **2014**, *5* (1), 3173.

https://doi.org/10.1021/acsphotonics.3c00983
ACS Photonics 2023, 10, 4038−4044